Polymorphic Signature of the Anti-inflammatory Activity of 2,2′-{[1,2-Phenylenebis(methylene)]bis(sulfanediyl)}bis(4,6-dimethylnicotinonitrile)

Rashmi Dubey,[†] Praveen Singh,[†] Ajeet K. Singh,[‡] Manoj K. Yadav,[§] D. Swati,[§] Manjula Vinayak,[‡] Carmen Puerta,[∥] Pedro Valerga,[∥] K. Ravi Kumar,[⊥] B. Sridhar,[⊥] and Ashish K. Tewari*,[†]

[†]Department of Chemistry, Faculty of Science, Banaras Hindu University, Varanasi 221005, India

[‡]Department of Zoology, Faculty of Science, Banaras Hindu University, Varanasi 221005, India

[§]Department of Bioinformatics, MMV, Banaras Hindu University, Varanasi 221005, India

[∥]Departamento de Ciencia de los, Materiales e Ingenieria Metalurgica, Facultad de Ciencias, Campus Universitario del Rio San Pedro, Puerto Real 11510, Spain

[⊥]Laboratory of X-ray Crystallography, Indian Institute of Chemical Technology, Hyderabad 500607, India

S *Supporting Information*

ABSTRACT: Weak noncovalent interactions are the basic forces in crystal engineering. Polymorphism in flexible molecules is very common, leading to the development of the crystals of same organic compounds with different medicinal and material properties. Crystallization of 2,2′-{[1,2-phenylenebis(methylene)]bis(sulfanediyl)}bis(4,6-dimethylnicotinonitrile) by evaporation at room temperature from ethyl acetate and hexane and from methanol and ethyl acetate gave stable polymorphs **4a** and **4b**, respectively, while in acetic acid, it gave metastable polymorph **4c**. The polymorphic behavior of the compound has been visualized through single-crystal X-ray and Hirshfeld analysis. These polymorphs are tested for anti-inflammatory activity via the complete Freund's adjuvant-induced rat paw model, and compounds have exhibited moderate activities. Studies of docking in the catalytic site of cyclooxygenase-2 were used to identify potential anti-inflammatory lead compounds. These results suggest that the supramolecular aggregate structure, which is formed in solution, influences the solid state structure and the biological activity obtained upon crystallization.
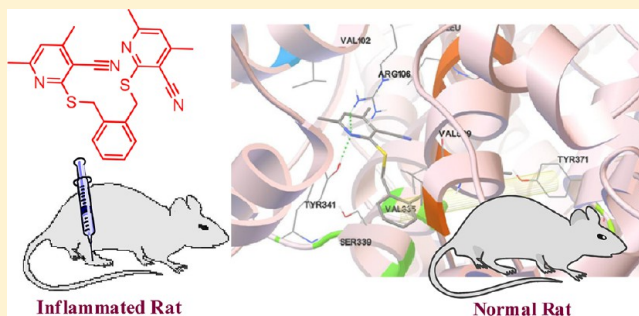
1. INTRODUCTION

Crystal polymorphism, which represents the ability of molecules to crystallize in more than one conformation displaying different physical and chemical properties, is of paramount importance in different fields such as pharmacy, solid state chemistry, and materials science.[1−5] It is well documented that polymorphism reveals the differences in pharmaceutically relevant properties, such as hygroscopicity, stability, solubility, dissolution rates, bioavailability, and sometimes biological activities.[6−8] According to Ostwald's rule of stages, polymorphs arise by emulative crystallization and development of metastable to stable polymorphic structures.[9,10] Once a metastable domain is encountered, kinetic pathways determine which form will crystallize.[11,12] The possibility of the establishment of noncovalent attractive interactions involving sulfur atoms from one side and oxygen or nitrogen atoms from the other has long been recognized.[13-15] These interactions play an important role in governing properties like spectroscopic behavior and chemical reactivity. In medicinal chemistry, special attention has been paid to the influence of such nonbonded interactions on the design of new drug candidates.[16]

Hydrogen bonding, CH···π, S···π,[17] and π−π, are important adhesive and cohesive forces in the crystallization of small aromatic molecules, which occurs between a soft acid and a soft base.[18,19] These interactions undoubtedly play important roles in determining the conformation of such molecules,[20] crystal packing,[21] the assembly of molecules into an organized supramolecular structure,[22] and the structure of proteins and DNA.[23]

Several examples of organosulfur compounds are known, whose conformations, geometries, and biological activity are influenced by intramolecular nonbonded sulfur−oxygen, sulfur−nitrogen, or sulfur−sulfur interactions.[24,25] In these molecules, the S···O, S···N, and S···S nonbonded distances are

significantly shorter than the sum of the corresponding van der Waals radii (3.32, 3.35, and 3.60 Å, respectively).

This work deals with the synthesis and development of polymorphs of the experimental flexible molecule 2,2′-{[1,2-phenylenebis(methylene)]bis(sulfanediyl)}bis(4,6-dimethylnicotinonitrile) (4). The impact of different polymorphs of 4 on the cyclooxygenase-2 (COX-2) receptor is experimentally justified by the evaluation of their anti-inflammatory activities. The different polymorphs were generated on the grounds of the difference in the polarity of solvents and the rate of cooling of the solution or evaporation of the solvent.

The synthesis of title compound 4 (Scheme 1) was conducted by first synthesizing 4,6-dimethyl-2-thioxo-1,2-

Scheme 1. Synthesis of 2,2′-[1,2-Phenylenebis(methylene)]bis(sulfanediyl)}bis(4,6-dimethylnicotinonitrile) (4)
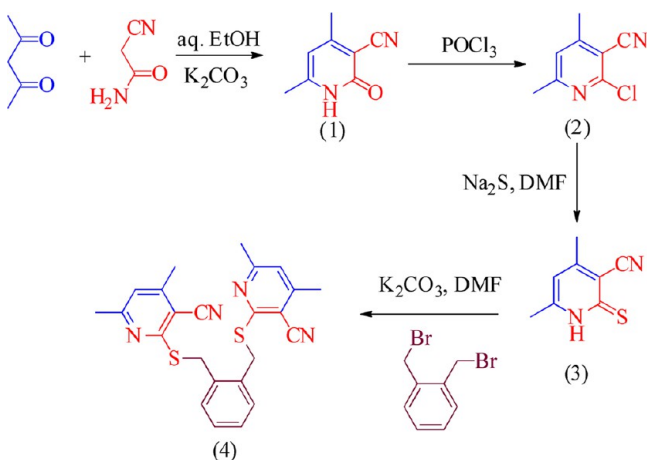
dihydropyridine-3-carbonitrile (3) by a general experimental procedure involving S_N2 reactions at room temperature. For the synthesis of compound 3, 4,6-dimethyl-2-oxo-1,2-dihydropyridine-3-carbonitrile (1) has been synthesized by the reaction of acetyl acetone and cyanoacetamide in an aqueous ethanolic solution of potassium carbonate. 2-Chloro-4,6-dimethylnicotinonitrile (2) has been synthesized from the reaction of phosphoryl chloride with compound 1,[26] which upon reaction with sodium sulfide in dimethylformamide (DMF) at room temperature in 5 h afforded compound 3.[27] Compound 3 upon reaction with 1,2-bis(bromomethyl)benzene (0.5 equiv) in K_2CO_3 and DMF yielded symmetrical 2,2′-{[1,2-phenylenebis-

(methylene)]bis(sulfanediyl)}bis(4,6-dimethylnicotinonitrile) (4).

2. EXPERIMENTAL SECTION

2.1. General Procedures. All reactions were monitored by thin layer chromatography (TLC) over silica gel G UV active plates. The melting points were recorded on an electrically heated block and are uncorrected. Infrared data were recorded as KBr discs on an Excalibur Series Bio-Rad Merlin FTS 3000 spectrophotometer. Nuclear magnetic resonance (NMR) spectra were recorded on Bruker Avance 300 MHz FT spectrometers equipped with a 5 mm dual probe and a 6 mm multinuclear inverse probe head with a Z-shielded gradient using TMS as an internal reference [chemical shift in δ (parts per million)]. Mass spectra of the compounds were recorded with a Jeol-JMS-D-300 instrument. Microanalysis was conducted on a Perkin-Elmer PE 2400 CHN elemental analyzer for dried samples.

2.2. Synthesis of 2,2′-[1,2-Phenylenebis(methylene)]bis-(sulfanediyl)}bis(4,6-dimethylnicotinonitrile) (4). In a 100 mL round-bottom flask, compound 3 (0.5 g, 0.003 mol) was dissolved in dry DMF and the mixture stirred for 15 min. Anhydrous potassium carbonate (0.46 g, 0.003 mol) was added and the mixture stirred for 2 h. 1,2-Bis-bromomethyl-benzene (0.44 g, 0.002 mol) was added to the mixture and left to stir for 20 h. Completion of the reaction was monitored via TLC. DMF was removed through a rotary evaporator, and ice-cold water was added. Precipitates appeared and were filtered with a Buchner funnel. The compound was recrystallized, which yielded an almost pure product: mp 236 °C; yield 0.8 g (67%); ^{1}H NMR (CDCl$_3$, 300 MHz) δ 2.41 (s, 6H, C<u>H</u>$_3$), 2.52 (s, 6H, C<u>H</u>$_3$), 4.68 (s, 4H, SC<u>H</u>$_2$), 6.77 (s, 2H, HetArC<u>H</u>), 7.19 (d, 2H, Ar-CH), 7.44 (d, 2H, Ar-CH); ^{13}C NMR (CDCl$_3$, 300 MHz) δ 20.08 (<u>C</u>H$_3$), 24.72 (<u>C</u>H$_3$), 28.90 (S<u>C</u>H$_2$), 29.10 (<u>C</u>H$_2$), 104.93 (<u>C</u>CN), 115.23 (<u>C</u>N), 119.73 (HetAr<u>C</u>H), 151.76 (<u>C</u>CH$_3$), 161.37 (<u>C</u>CH$_3$), 161.97 (<u>C</u>SC); IR (KBr, cm^{-1}) 613−870 (C−H bending), 1412−1579 (C═C, aromatic stretching), 2217 (C−N stretching), 2855−2924 (C−H stretching); FAB MS m/z 430 (M + 1). Elemental analysis for C$_{24}$H$_{23}$N$_4$S$_2$. Calcd: C, 66.94; H, 5.15; N, 13.01. Found: C, 66.89; H, 5.09; N, 12.99.

2.3. Crystallization Experiments. *Polymorph 4a.* 2,2′-{[1,2-Phenylenebis(methylene)]bis(sulfanediyl)}bis(4,6-dimethylnicotinonitrile) was crystallized in a mixture of ethyl acetate and hexane (2:1) by slow evaporation at room temperature to afford cocrystal 4a.

Polymorph 4b. Again, 2,2′-{[1,2-phenylenebis(methylene)]bis-(sulfanediyl)}bis(4,6-dimethylnicotinonitrile) was crystallized in a mixture of methanol and ethyl acetate (2:0.5) by slow evaporation at room temperature to afford cocrystal 3b, having slight differences in bond angles.

Polymorph 4c. Again, 2,2′-{[1,2-phenylenebis(methylene)]bis-(sulfanediyl)}bis(4,6-dimethylnicotinonitrile) was crystallized in a mixture of acetic acid by slow evaporation at room temperature to afford cocrystal 3c, having more differences in bond angles.
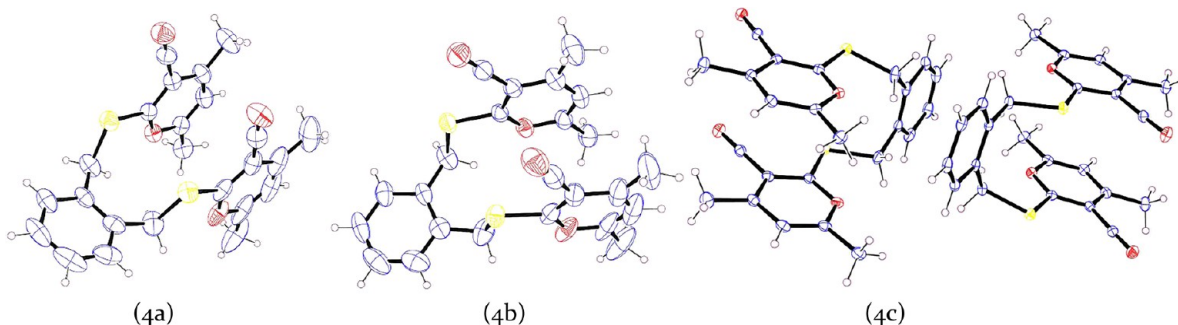
Figure 1. ORTEP drawing of the polymorphs of 2,2′-{[1,2-phenylenebis(methylene)]bis(sulfanediyl)}bis(4,6-dimethylnicotinonitrile) in different solvents: **4a** from ethyl acetate and hexane (2:1), **4b** from methanol and ethyl acetate (2:0.5), and **4c** from acetic acid at 50% thermal ellipsoid probabilities.

2.4. X-ray Crystallography. Single-crystal X-ray data, space groups, unit cell dimensions, and intensity data for **4a**−**4c** were collected with an Oxford Diffraction X-calibur CCD diffractometer using graphite monochromated Mo Kα radiation ($\lambda = 0.71073$ Å). The structures were determined by direct methods using SHELXS-97[28] and refined on F^2 by a full-matrix least-squares technique using SHELXL-97. Non-hydrogen atoms were refined anisotropically, and hydrogen atoms were geometrically fixed with thermal parameters equivalent to 1.2 times that of the atom to which they are bonded. Molecular diagrams (Figure 1) for all polymorphs were prepared using ORTEP,[29] and the packing diagrams were generated using Mercury version 3.1. PLATON[30] was used for the analysis of bond lengths, bond angles, and other geometrical parameters. Hirshfeld surface analysis was conducted to make quantitative evaluations between contributions of different noncovalent interactions in polymorphs.[31,32] Other crystallographic data are summarized in Table 1.

Table 1. Crystallographic Details of 2,2′-{[1,2-Phenylenebis(methylene)]bis(sulfanediyl)}bis(4,6-dimethylnicotinonitrile) Polymorphs 4a−4c

	4a	4b	4c
empirical formula	$C_{24}H_{22}N_4S_2$	$C_{24}H_{22}N_4S_2$	$C_{24}H_{22}N_4S_2$
formula weight	430.58	430.58	430.58
crystal system	monoclinic	monoclinic	monoclinic
space group	$P2_{1/n}$	$P2_{1/n}$	$P2_{1/c}$
unit cell dimensions			
a (Å)	10.667(2)	10.6469(10)	15.815(3)
b (Å)	18.767(4)	18.7554(17)	18.657(4)
c (Å)	11.252(2)	11.2374(10)	14.626(3)
β (deg)	93.53(3)	93.539(2)	92.98(3)
V (Å^3)	2248.1(8)	2239.68	4309.8(15)
Z	4	4	8
μ (mm)	0.255	0.256	0.266
hkl ranges	$-12 \leq h \leq 12$	$-12 \leq h \leq 12$	$-21 \leq h \leq 20$
	$-22 \leq k \leq 21$	$-22 \leq k \leq 22$	$-20 \leq k \leq 25$
	$-13 \leq l \leq 13$	$-13 \leq l \leq 13$	$-20 \leq l \leq 18$
R factor (%)	6.02	5.32	5.63
CCDC No.	710839	973582	722257

3. RESULTS AND DISCUSSION

2,2′-{[1,2-Phenylenebis(methylene)]bis(sulfanediyl)}bis(4,6-dimethylnicotinonitrile) (Figure 2) was crystallized in a mixture
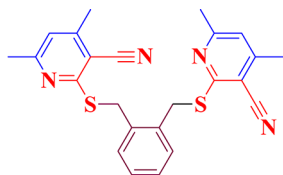
Figure 2. Molecular structure of 2,2′-{[1,2-phenylenebis(methylene)]-bis(sulfanediyl)}bis(4,6-dimethylnicotinonitrile).

of ethyl acetate and hexane (2:1) by slow evaporation at room temperature and yielded good quality crystals (**4a**). Another polymorph, **4b**, was crystallized in a mixture of methanol and ethyl acetate (2:0.5) by slow evaporation at room temperature, having slight differences in bond angles. Polymorph **4c** was crystallized in acetic acid, resulting in two conformations with different symmetry elements.

Polymorph **4a** crystallized in the $P2_{1/n}$ monoclinic space group with the following values: $a = 10.667(2)$ Å, $b = 18.767(4)$ Å, $c = 11.252(2)$ Å, $\beta = 93.53(3)°$, $Z = 4$, and $V = 2248.1(8)$ Å. Polymorph **4b** crystallized in the $P2_{1/n}$ monoclinic space group with the following values: $a = 10.6469(10)$ Å, $b = 18.7554(17)$ Å, $c = 11.2374(10)$ Å, $\beta = 93.539(2)°$, $Z = 4$, and $V = 2239.6(8)$ Å. In both polymorphs **4a** and **4b**, there is slight difference in bond angles and bond lengths. Polymorph **4c** crystallized in the $P2_{1/c}$ monoclinic space group with the following values: $a = 15.815(3)$ Å, $b = 18.657(4)$ Å, $c = 14.626(3)$ Å, $\beta = 92.98(3)°$, $Z = 8$, and $V = 4309.8(15)$ Å (Table 1).

In polymorphs **4a** and **4b**, the mean separations between two stacked pyridine rings are 3.932 and 3.937 Å, respectively. In the case of polymorph **4c**, the mean separations between two stacked pyridine rings are 3.905 and 3.829 Å (Table 2). In both polymorphs **4a** and **4b**, the angles between two 3-cyano, 4,6-dimethyl-2-thio-nicotinonitrile ring planes are 1.95° and 4.59°, respectively, whereas in polymorph **4c**, the angle between two types of 3-cyano, 4,6-dimethyl-2-thio-nicotinonitrile ring planes is 3.16°, as shown in Figure S1 of the Supporting Information.

Intramolecular and intermolecular $\pi-\pi$ interactions create the molecular stability in the parallel conformation. Packing of the molecule has been stabilized via various weak interactions. In the packing diagram of polymorph **4a**, all 3-cyano, 4,6-dimethyl-2-thio-nicotinonitrile rings are parallel to each other because of the presence of intramolecular $\pi\cdots\pi$ (3.932 Å) and intermolecular $\pi\cdots\pi$ (3.742 Å) interactions. This arene interaction is also observed in the packing diagram of polymorph **4b**, while in the packing diagram of polymorph **4c**, the parallel motif is stabilized by two types of intramolecular $\pi\cdots\pi$ interactions (3.905 and 3.829 Å) and also by two types of intermolecular $\pi\cdots\pi$ interactions (3.905 and 3.571 Å) .

In crystals **4a**−**4c**, the intramolecular edge to face C−H⋯π, C−H⋯N, and C−H⋯S groups also stabilized the conformation of polymorphs **4a** and **4b**, which have slight differences in their bond lengths and bond angles. However, intramolecular CH⋯N and $\pi\cdots\pi$ interactions stabilized the conformation of one of the conformers in crystal **4c**, while the other was stabilized by S⋯S interaction along with such interaction as shown in Figure 3. Hirshfeld surface analysis (Figure 4) shows the contributions of all hydrogens and interactions in polymorphs **4a** and **4b** are the same but those in **4c** are different because of the different extents of inter- and intramolecular interactions. The sharp spikes in the fingerprint plot of **4a** and **4b** at de = di ≈ 1.1 Å indicate short $\pi\cdots\pi$ interactions in comparison to those of **4c**.

Powder X-ray diffraction (XRD) analysis of polymorphs **4a** and **4b** reveals that they show the same pattern, while **4c** shows a different pattern that indicates a new polymorph of compound 2,2′-{[1,2-phenylenebis(methylene)]bis-(sulfanediyl)}bis(4,6-dimethylnicotinonitrile) as shown in Figure 5.

3.1. Cox-2 _In Silico_ Studies of Polymorphs. _Auto Dock Protocol._ First, all bound waters, ligands, and cofactors were removed from the proteins. The macromolecule was checked for polar hydrogens; torsion bonds of the inhibitors were selected and defined. Gasteiger charges were computed, and the Auto Dock atom types were defined using Auto Dock version 4.2, the graphical user interface of Auto Dock supplied by MGL Tools.[33] The Lamarckian genetic algorithm (LGA), which is considered one of the best docking methods available in Auto Dock,[34,35] was employed. This algorithm yields superior docking performance compared to simulated annealing or the

Table 2. Weak Interactions and Intramolecular Atomic Distances in Polymorphic Cocrystals 4a−4c of 2,2′-{[1,2-Phenylenebis(methylene)]bis(sulfanediyl)}bis(4,6-dimethylnicotinonitrile)

crystal	interaction	d (Å)	D (Å)	θ (deg)	crystal	interaction	d (Å)	D (Å)	θ (deg)
4a	C24−H24B···S1	0.960(5)	2.814	139.51		C13−H13A···N2	0.971(3)	2.566	92.06
	C8−H8C···N2	0.960(3)	2.733	163.08		C13−H13B···N2	0.970(3)	2.72	83.1
	C9−H9B···S2	0.970(4)	3.533	95.11		C6−H6A···N1	0.970(3)	3.426	50.96
	C7−H7A···π	0.961(5)	3.718	153.77		C6−H6B···N1	0.971(3)	2.350	116.35
	C7−H7C···N3	0.959(5)	3.791	117.27	**4c**	C16−H16A···π	0.991(3)	3.245	147.42
	π···π (intramolecular)		3.937			C9−H9A···π	0.990(3)	3.652	87.97
	π···π (intermolecular)		3.747			C9−H9B···π	0.991(2)	3.082	125.90
	C8−H8A···π	0.959(4)	3.47	103.65		C33−H33A···π	0.990(2)	3.769	87.80
	C4−H4···π	0.930(4)	3.288	168.20		C33−H33B···π	0.991(2)	3.218	123.97
	C24−H24A···π	0.960(7)	3.86	88.01		C40−H40A···π	0.990(2)	3.499	134.39
	C24−H24B···π	0.960(5)	3.712	96.92		S1···S2		3.551	
	C6−N2···S2	1.145(5)	3.831	82.05		S3···S4		3.736	
	C16−H16B···N2	0.970(4)	3.368	123.83		C9−H9A···N1	0.990(3)	3.333	56.31
	C8−H8B···S2	0.960(3)	3.132	155.26		C9−H9B···N1	0.991(2)	2.364	113.37
	S1···S2		3.666			C16−H16A···N3	0.991(3)	2.472	99.42
4b	C20−H20A···C9	0.960(4)	2.845	158.95		C16−H16B···N3	0.990(3)	2.896	75.12
	C22−H22B···S1	0.960(4)	2.855	134.88		C33−H33A···N5	0.990(2)	2.750	84.52
	C19−H19C···N3	0.960(3)	2.724	162.88		C33−H33B···N5	0.991(2)	2.677	88.68
	C19−H19B···S2	0.960(3)	3.124	155.23		C40−H40A···N7	0.990(2)	2.322	117.00
	C22−H22C···N4	0.960(4)	2.772	155.60		C40−H40B···N7	0.989(2)	3.490	47.06
	C20−H20B···C21	0.960(4)	2.732	88.09		N1···S2		3.733	
	C20−H20C···C21	0.960(4)	2.885	79.24		N7···S3		3.681	
	C23−H23B···C24	0.960(5)	2.735	91.17		C8−H8A···N3	0.980(2)	3.087	135.47
	S1···S2		3.658			C48−H48B···N5	0.980(2)	3.855	69.81
	C6−H6B···S2	0.971(3)	3.54	94.75		C48−H48C···N5	0.980(2)	2.985	124.8
	C13−H13A···S1	0.971(3)	3.622	93.17		C16−H16A···N1	0.991(3)	3.491	117.97
	C19−H19A···N2	0.960(3)	3.094	126.55		C9−H9B···N3	0.991(2)	3.875	141.27
	π···π (intramolecular)		3.932			C33−H33B···N7	0.991(2)	2.884	131.91
	π···π (intermolecular)		3.742			C47−H47C···N6	0.981(2)	3.346	134.60
	C3−H3···π	0.930(3)	3.280	167.85		π···π (intramolecular)		3.905	
	C20−H20A···π	0.960(4)	3.705	154.35		π···π (intramolecular)		3.829	
	C20−H20B···N3	0.960(4)	3.207	101.8		C16−H16A···S1	0.991(3)	3.846	85.06
	C20−H20C···N3	0.960(4)	3.392	90.39		C9−H9B···S2	0.991(2)	3.299	98.54
	C20−H20B···N4	0.960(4)	3.294	133.87		C8−H8A···π	0.980(2)	3.170	116.12
	C19−H19A···N4	0.960(3)	3.497	105.55		C44−H44···π	0.950(2)	3.873	73.77
	C19−H19B···N4	0.960(3)	3.684	93.75		C48−H48B···π	0.980(2)	3.793	84.82
	C19−H19C···N4	0.960(3)	3.812	86.11		C40−H40A···S3	0.990(2)	3.680	92.11
	C23−H23A···N3	0.959(5)	3.492	149.16		C33−H33B···S4	0.991(2)	3.585	96.02
	C23−H23B···N4	0.960(5)	3.259	105.17		π···π (intermolecular)		3.905	
	C23−H23C···N4	0.959(5)	3.571	85.84		π···π (intermolecular)		3.571	
	C19−H19A···π	0.960(3)	3.456	104.58		C40−H40B···N6	0.989(2)	3.523	134.04
	C19−H19B···π	0.960(3)	3.779	84.76		C37−H37···N6	0.950(2)	2.679	164.07
	C22−H22A···N2	0.960(7)	2.415	77.76		C38−H38···N8	0.950(2)	2.831	162.39
	C22−H22B···N2	0.960(4)	3.096	48.12		C23−H23C···N8	0.980(3)	3.930	111.95
	C22−H22C···N2	0.961(4)	2.934	37.16		C47−H47B···N4	0.979(3)	3.270	84.90
	C24···S2		2.965			C24−H24B···S4	0.980(2)	2.952	131.65
	C21···S1		2.972			C24−H24C···S4	0.981(2)	3.522	91.30
	C22−H22C···S2	0.961(4)	3.872	134.85		C20−H20···N8	0.949(2)	2.926	154.26
	C19−H19B···S1	0.960(3)	3.686	111.97		C23−H23B···S1	0.980(3)	3.652	120.12
	C19−H19C···S1	0.960(3)	3.713	110.05					

simple genetic algorithm and the other search algorithms available in Auto Dock version 4.0. Second, the three-dimensional grid boxes were created by the Auto Grid algorithm to evaluate the binding energies on the macro-molecule coordinates. The grid maps representing the intact ligand in the actual docking target site were calculated with Auto Grid (part of the Auto Dock package). Eventually, cubic grids encompassed the binding site where the intact ligand was

embedded. Finally, Auto Dock was used to calculate the binding free energy of a given inhibitor conformation in the macromolecular structure, while the probable structural inaccuracies were ignored in the calculations. The search was extended over the whole receptor protein used as blind docking. Molecular docking of compounds was conducted in the COX-2 crystal structure of Protein Data Bank (PDB) entry 3LN1 (2.9 Å resolution). Celecoxib and nimesulide as COX-2

1350

dx.doi.org/10.1021/cg401842y | *Cryst. Growth Des.* 2014, 14, 1347−1356

(4a)

(4b)

(4c)
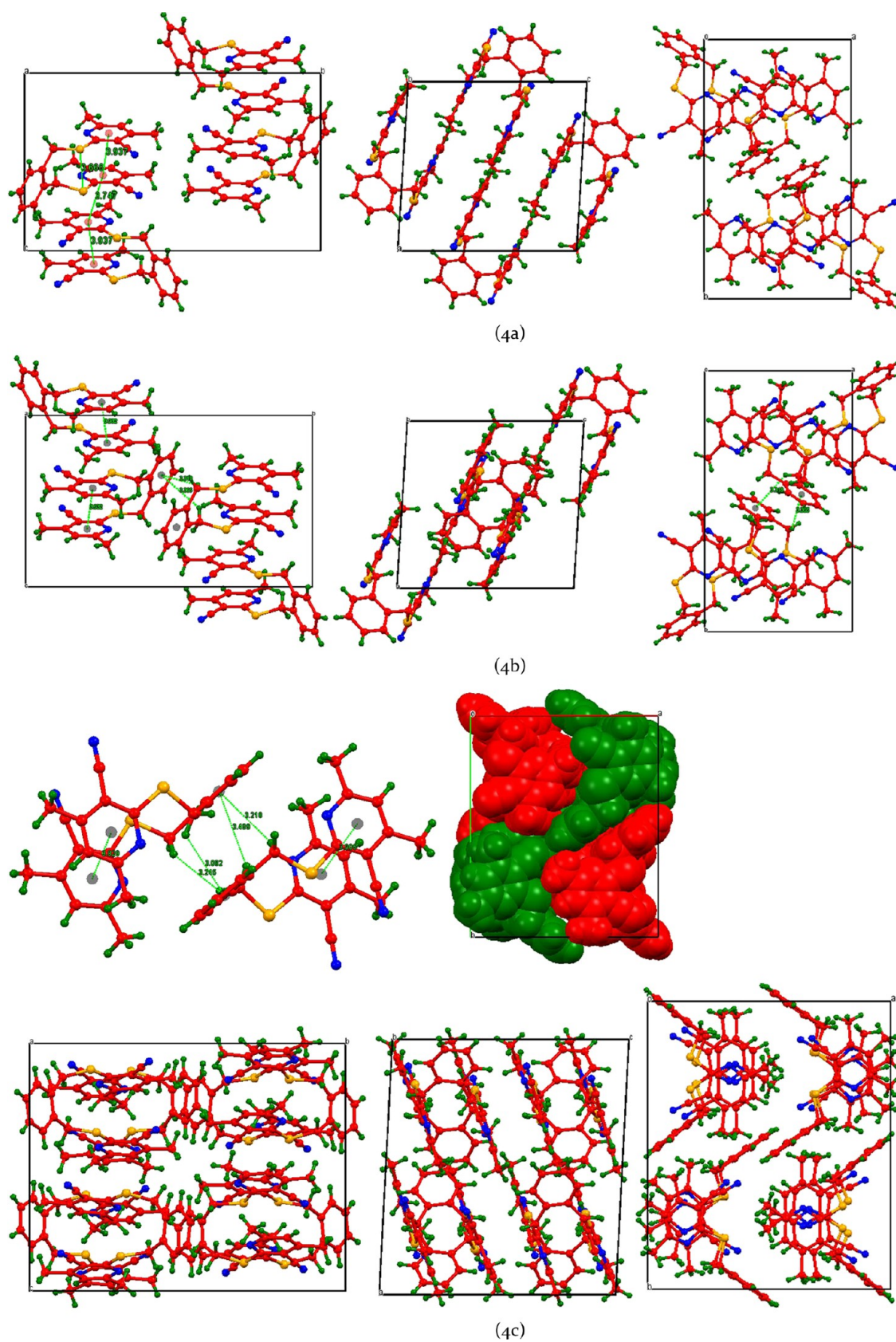
Figure 3. Views of the structure of polymorphs of 2,2′-{[1,2-phenylenebis(methylene)]bis(sulfanediyl)}bis(4,6-dimethylnicotinonitrile) (**4a**) grown from ethyl acetate and hexane (2:1), **4b** grown from methanol and ethyl acetate (2:0.5), and **4c** grown from acetic acid along *a*, *b*, and *c* axes. Hydrogen bonds are represented by broken light green lines. Carbon atoms are colored red, hydrogen atoms green, sulfur atoms orange, and nitrogen atoms blue.
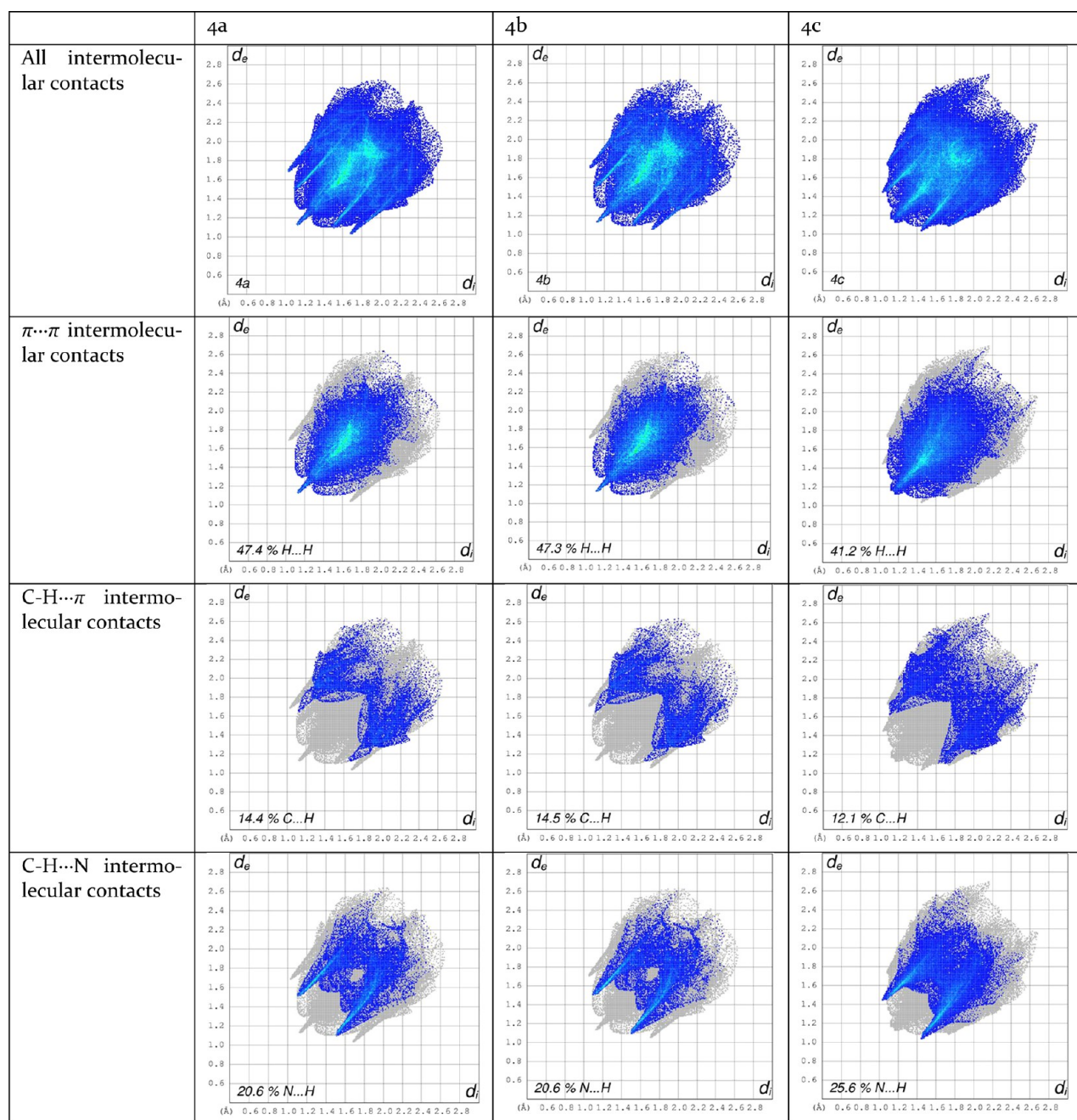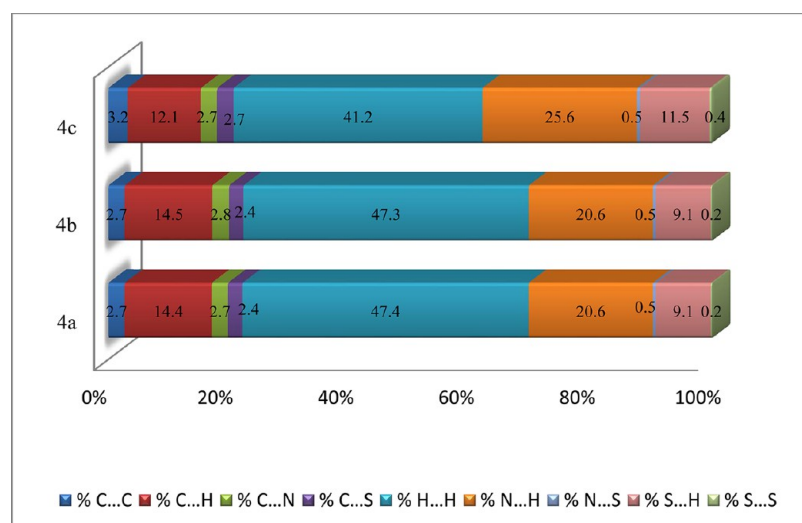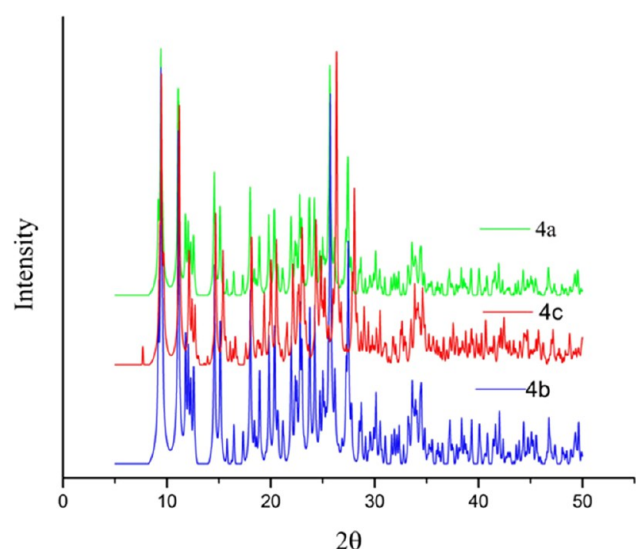
	4a	4b	4c
All intermolecular contacts			
$\pi\cdots\pi$ intermolecular contacts			
C-H$\cdots\pi$ intermolecular contacts			
C-H$\cdots$N intermolecular contacts			

Figure 4. continued

Figure 4. Hirshfeld surface two-dimensional fingerprint plots for the different intermolecular interactions in polymorphs **4a−4c** of 2,2′-{[1,2-phenylenebis(methylene)]bis(sulfanediyl)}bis(4,6-dimethylnicotinonitrile).

Figure 5. Powder XRD of crystals **4a−4c**.

selective drugs (native ligand) in the crystal structure were also docked as references. Table 3 shows the docking scores of

**Table 3. Docking Scores of Polymorphs 4a−4c, Celecoxib, and Nimesulide with the COX-2 Protein (PDB entry 3LN1)**

compound	binding energy (kcal/mol)
celecoxib	−10.83
nimesulide	−12.09
4a	−10.76
4b	−11.74
4c	−10.79

polymorphs **4a−4c** within the active sites of COX-2 (Figure 6a). From the docking score, it is apparent that **4b** shows a better binding affinity with COX-2 than **4a** and **4c**. COX-2 has the larger active site, which makes it possible for molecules to fit into the COX-2 active site versus the COX-1 channel. The larger active site of COX-2 is partly due to an additional polar hydrophilic side pocket compared to that of COX-1. Thus, it is thought to be a key residue for diaryl heterocycle inhibitors

such as the coxibs. The bulky sulfonamide group in COX-2 inhibitors such as celecoxib prevents the molecule from entering the COX-1 channel. In celecoxib, the lipophilic pocket is unavailable by an optionally substituted phenyl ring or a bulky alkoxy substituent. Within the hydrophilic side pocket of COX-2, the oxygen of the sulfonamide group forms hydrogen bonds. The substituted phenyl group at the top of the channel interacts with the side chains of amino acid residues through hydrophobic and electrostatic interactions (Figure 6b). The docking study reveals that compound **4** structurally resembles celecoxib. Therefore, the anti-inflammatory activity of compound **4** is tested by our *in vivo* study in rats and compared with that of the commercial drug nimesulide.

3.2. Biological Activity. *Materials and Methods.* The anti-inflammatory activity of compounds was evaluated by the complete Freund's adjuvant (CFA)-induced rat paw edema method. The rat colony was maintained as per norms of the institutional animal ethical committee, at 25 ± 2 °C under 12 h light/dark schedules with *ad libitum* supply of food and water. Experiments were performed on adult (12−13 weeks) male rats, weighting 130−150 g. Paw edema was induced by subcutaneous injection of 100 μL of 1 mg/mL CFA (Sigma-Aldrich) in the plantar surface of the right hind paws of rats. Rats were divided into five groups, having five rats in each group. One group was kept as a control. Group 2 was treated with the standard NSAID nimesulide. Groups 3−5 were treated with synthesized compounds **4a−4c**, respectively. A single dose of each drug (10 mg/kg of body weight) was given through intraperitoneal injection. The dorso-ventral thickness of the hind paw was measured by using a Vernier caliper placed at the border of the phalanges and metatarsals. An increase in paw thickness was compared with that of normal mice. Measurements were taken 2, 6, and 24 h after CFA injection. Each measurement was repeated three times. The percentage increase in paw thickness was calculated using the formula $[(t - t_0)/t_0] \times 100$, where t_0 and t are the thicknesses of the paw before and after CFA injection, respectively.

The percentage inhibition of swelling was calculated by the formula $(C - T/C) \times 100$, where C and T are the increases in the paw thickness of the control and drug-treated groups, respectively.
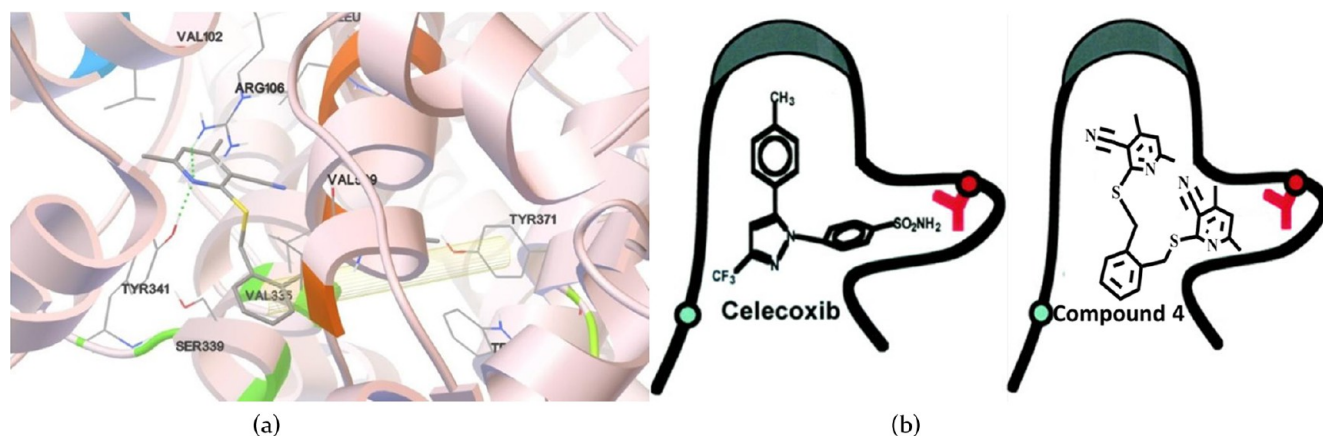
Figure 6. (a) Docked pose of compound **4b** within COX-2 (PDB entry 3LN1). (b) Structure–activity relationship of celecoxib and compound **4** with the COX-2 active site.

Statistical Analysis. The results are expressed as means ± standard error of the mean (SEM). The data were analyzed using one-way analysis of variance (ANOVA), followed by Tukey's post hoc test. A p value of <0.05 was considered to be statistically significant (Figure 7). The percentage increases in paw thickness at different time intervals (mean ± SEM) are listed in Table 4.
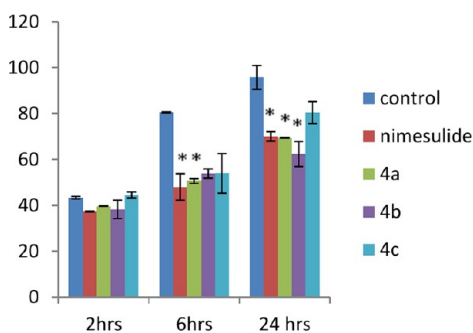
Figure 7. Effect of synthesized compounds on paw thickness 2, 6, and 24 h after CFA injection. Values are expressed as means ± SEM. An asterisk indicates a significant difference from the control group at the $p < 0.05$ level of significance using a one-way ANOVA followed by Tukey's post hoc test.

From the anti-inflammatory activity, it was observed that all the compounds are ineffective at the 2 h time point. After 6 h, compounds **4a** and **4b** showed anti-inflammatory activity (levels of inhibition of paw edema of 37.12 and 33.10%, respectively), which was lower than that of the positive control nimesulide (40.44% inhibition). At 24 h, the anti-inflammatory activity of **4a** and **4b** was slightly better (27.54 and 34.92%, respectively) than that of nimesulide (26.89%). On average, **4a** shows better anti-inflammatory activity than **4b**. Compound **4c**

does not show anti-inflammatory activity at any time point. The better activity of these compounds in the late phase may be due to slow absorption or delayed action of compounds **4a** and **4b** compared to that of nimesulide. A pharmacokinetic study is needed to resolve these issues.

4. CONCLUSION

Hydrogen bonding is important in crystallization. The stoichiometry of the solvent influenced π-stacking motifs in 2,2′-{[1,2-phenylenebis(methylene)]bis(sulfanediyl)}bis(4,6-dimethylnicotinonitrile) that make finite and infinite aromatic stacks. In our studies, it is noted that the crystallization of a compound in different solvents induces different noncovalent interactions such as sulfur–sulfur, C–H···π, C–H···N, and C–H···S interactions and is responsible for the formation of different polymorphic crystals. Structural investigations of the relationship between crystallization and novel polymorph discovery should be interesting given the immense importance of these solid state substances in the pharmaceutical industry. This study represents the COX-2 activity of polymorphs **4a**–**4c**. Among them, **4a** and **4b** are much more potent with respect to anti-inflammatory activity, which attracts interest in the polymorphs for their diverse biological activities such as anti-inflammatory, anticancer, analgesic, antihypertensive, antihistamine, etc. These are matters that need to be resolved with further experimentation and/or modeling.

■ ASSOCIATED CONTENT

ⓢ Supporting Information

ORTEP and cif files of polymorphs **4a**–**4c**. This material is available free of charge via the Internet at http://pubs.acs.org.

Table 4. Percentage Increases in Paw Thickness at 2, 6, and 24 h Intervals (mean ± SEM) and Average Levels of Inhibition of Edema at Different Time Intervals

	2 h	6 h	24 h	average level of inhibition of edema (%) at different time intervals
control	43.3 ± 0.53	80.45 ± 0.18	95.75 ± 5.16	–
nimesulide	37.3 ± 0.16	47.91 ± 5.76	70 ± 2.041	27.06
4a	39.60 ± 0.18	50.58 ± 1.01	69.38 ± 0.17	24.40
4b	38.22 ± 3.99	53.82 ± 2.03	62.31 ± 5.49	26.58
4c	44.47 ± 1.29	53.92 + 8.62	80.31 ± 4.82	15.45

■ AUTHOR INFORMATION

Corresponding Author

*E-mail: ashishtewarichem@gmail.com.

Author Contributions

R.D. and P.S. contributed equally to this work. A.K.S. performed biological activity experiments in supervision of M.V.

Notes

The authors declare no competing financial interests.

■ REFERENCES

(1) Bernstein, J. *Polymorphism in Molecular Crystals*; Clarendon Press: Oxford, U.K., 2002.

(2) Bernstein, J. *Conformational Polymorphism in Solid State Chemistry*; Desiraju, G. R., Ed.; Elsevier: Amsterdam, 1987.

(3) Brittain, H. G. *Polymorphism in Pharmaceutical Solids*; Marcel Dekker: New York, 1999; p 95.

(4) Bernstein, J. *Chem. Commun.* **2005**, 5007.

(5) Dunitz, J. D.; Bernstein, J. *Acc. Chem. Res.* **1995**, *28*, 193.

(6) Cheney, M. L.; Shan, N.; Healey, E. R.; Hanna, M.; Wojtas, L.; Zaworotko, M. J.; Sava, V.; Song, S. J.; Sanchez-Ramos, J. R. *Cryst. Growth Des.* **2010**, *10*, 394−405.

(7) Roy, S.; Quiñones, R.; Matzger, A. J. *Cryst. Growth Des.* **2012**, *12* (4), 2122−2126.

(8) Zimmermann, A.; Frostrup, B.; Bond, A. D. *Cryst. Growth Des.* **2012**, *12*, 2961−2968.

(9) Ostwald, W. Z. *Phys. Chem.* **1897**, *22*, 289−330.

(10) Bernstein, J.; Davey, R. J.; Henck, J. O. *Angew. Chem., Int. Ed.* **1999**, *38*, 3440−3461.

(11) Miller, J. M.; Blackburn, A. C.; Macikenas, D. M.; Collman, B. C.; Rodríguez-Hornedo, N. Solvent Systems for Crystallization and Polymorph Selection. In *Solvent Systems and Their Selection in Pharmaceutics and Biopharmaceutics*; Augustins, P., Brewster, M. E., Eds.; AAPS Press: Arlington, VA, 2006.

(12) Weissbuch, I.; Addadi, L.; Leiserowitz, L. *Science* **1991**, *253*, 637−645.

(13) Addadi, L.; Berkovitch-Yellin, Z.; Weissbuch, I.; Mil, J. V.; Shimoa, L. J. W.; Lahav, M.; Leiserowitz, L. *Angew. Chem., Int. Ed.* **1985**, *24*, 466−485.

(14) Weissbuch, I.; Torbeev, V. Y.; Leiserowitz, L.; Lahav, M. *Angew. Chem., Int. Ed.* **2005**, *44*, 3226−3229.

(15) (a) Minyaev, R. M.; Minkin, V. I. *Can. J. Chem.* **1998**, *76*, 776−787. (b) Ohkata, K.; Ohsugi, M.; Yamamoto, K.; Ohsawa, M.; Akiba, K. *J. Am. Chem. Soc.* **1996**, *118*, 6355−6369. (c) Barton, D. H. R.; Hall, M. B.; Lin, Z.; Parekh, S. I.; Reibenspies, J. *J. Am. Chem. Soc.* **1993**, *115*, 5056−5059. (d) Pandya, N.; Basile, A. J.; Gupta, A. K.; Hand, P.; MacLaurin, C. L.; Mohammad, T.; Ratemi, E. S.; Gibson, M. S.; Richardson, M. F. *Can. J. Chem.* **1993**, *71*, 561−571.

(16) (a) Hirata, T.; Nomiyama, J.; Sakae, N.; Nishimura, K.; Yokomoto, M.; Inoue, S.; Tamura, K.; Okuhira, M.; Amano, H.; Nagao, Y. *Bioorg. Med. Chem. Lett.* **1996**, *6*, 1469−1474. (b) Hirata, T.; Shiro, M.; Nagao, Y. *Heterocycles* **1997**, *44*, 133−138. (c) Hirata, T.; Goto, S.; Tamura, K.; Okuhira, M.; Nagao, Y. *Bioorg. Med. Chem. Lett.* **1997**, *7*, 385−388. (d) Wexler, R. R.; Greenlee, W. J.; Irvin, J. D.; Goldberg, M. R.; Prendergast, K.; Smith, R. D.; Timmermans, P. B. M. W. M. *J. Med. Chem.* **1996**, *39*, 625−656.

(17) (a) Morgan, R. S.; McAdon, J. M. *Int. J. Pept. Protein Res.* **1980**, *15*, 177−180. (b) Morgan, R. S.; Tatsch, C. E.; Gushard, R. H.;

McAdon, J. M.; Warme, P. K. *Int. J. Pept. Protein Res.* **1978**, *11*, 209−217.

(18) Desiraju, G. R. *Acc. Chem. Res.* **2002**, *35*, 565−573.

(19) (a) Nishio, M.; Hirota, M.; Umezawa, Y. *The CH/π Interaction: Evidence, Nature and Consequences*; Wiley: New York, 1998. (b) Nishio, M.; Umezawa, Y.; Hirota, M.; Takeuchi, Y. *Tetrahedron* **1995**, *51*, 8665−8701.

(20) (a) Takahashi, O.; Yasunaga, K.; Gondoh, Y.; Kohno, Y.; Saito, K.; Nishio, M. *Bull. Chem. Soc. Jpn.* **2002**, *75*, 1777−1783. (b) Evans, D. J.; Junk, P. C.; Smith, M. K. *New J. Chem.* **2002**, *26*, 1043−1048. (c) Kitamura, M.; Nakano, K.; Miki, T.; Okada, M.; Noyori, R. *J. Am. Chem. Soc.* **2001**, *123*, 8939−8950. (d) Matusgi, M.; Itoh, K.; Nojima, M.; Hagimoto, Y.; Kita, Y. *Tetrahedron Lett.* **2001**, *42*, 8019−8022. (e) Tsuzuki, S.; Houjou, H.; Nagawa, Y.; Hiratani, K. *J. Chem. Soc., Perkin Trans. 2* **2001**, 1951−1955.

(21) (a) Bond, A. D. *Chem. Commun.* **2002**, 1664−1665. (b) Thuéry, P.; Asfari, Z.; Nierlich, M.; Vicens, J. *Acta Crystallogr.* **2002**, *C58*, 223−225. (c) Venkatraman, S.; Anand, V. G.; PrabhuRaja, V.; Rath, H.; Sankar, J.; Chandrashekar, T. K.; Teng, W.; Senge, K. R. *Chem. Commun.* **2002**, 1660−1661. (d) Takahashi, O.; Kohno, Y.; Iwasaki, S.; Saito, K.; Iwaoka, M.; Tomoda, S.; Umezawa, Y.; Tsuboyama, S.; Nishio, M. *Bull. Chem. Soc. Jpn.* **2001**, *74*, 2421−2430. (e) Adams, H.; Bernad, P. L., Jr.; Eggleston, D. S.; Haltiwanger, R. C.; Harris, K. D. M.; Hembury, G. A.; Hunter, C. A.; Livingstone, D. J.; Kariuki, B. M.; McCabe, J. F. *Chem. Commun.* **2001**, 1500−1501.

(22) (a) Yoshitake, Y.; Misaka, J.; Setoguchi, K.; Abe, M.; Kawaji, T.; Eto, M.; Harano, K. *J. Chem. Soc., Perkin Trans. 2* **2002**, 1611−1619. (b) Suezawa, H.; Yoshida, T.; Hirota, M.; Takahashi, H.; Umezawa, Y.; Honda, K.; Tsuboyama, S.; Nishio, M. *J. Chem. Soc., Perkin Trans. 2* **2001**, 2053−2058. (c) Tomura, M.; Yamashita, Y. *Chem. Lett.* **2001**, 532−533. (d) Piatnitski, E. L.; Flowers, R. A., II; Deshayes, K. *Chem.—Eur. J.* **2000**, *6*, 999−1006. (e) Takahashi, H.; Tsuboyama, S.; Umezawa, Y.; Honda, K.; Nishio, M. *Tetrahedron* **2000**, *56*, 6185−6191. (f) Watanabe, N.; Furusho, Y.; Kihara, N.; Takata, T.; Kinbara, K.; Saigo, K. *Bull. Chem. Soc. Jpn.* **2001**, *74*, 149−155. (g) Furusho, Y.; Shoji, J.; Watanabe, N.; Kihara, N.; Adachi, T.; Takata, T. *Bull. Chem. Soc. Jpn.* **2001**, *74*, 139−147. (h) Cabezon, B.; Cao, J.; Raymo, F. M.; Stoddart, J. F.; White, A. J. P.; Williams, D. J. *Chem.—Eur. J.* **2000**, *6*, 2262−2273. (i) Ashton, P. R.; Baldoni, V.; Balzani, V.; Claessens, C. G.; Credi, A.; Hoffmann, H. D. A.; Raymo, F. M.; Stoddart, J. F.; Venturi, M.; White, A. J. P.; Williams, D. J. *Eur. J. Org. Chem.* **2000**, 1121−1130.

(23) (a) Umezawa, Y.; Nishio, M. *Nucleic Acids Res.* **2002**, *30*, 2183−2192. (b) Kinoshita, T.; Miyake, H.; Fujii, T.; Shoji, T.; Goto, T. *Acta Crystallogr.* **2002**, *D58*, 622−626. (c) Weiss, M. S.; Brandl, M.; Sühnel, J.; Pal, D.; Hilgenfeld, R. *Trends Biochem. Sci.* **2001**, *26*, 521−523. (d) Brandl, M.; Weiss, M. S.; Jabs, A.; Sühnel, J.; Hilgenfeld, R. *J. Mol. Biol.* **2001**, *307*, 357.

(24) Kucsman, A.; Kapovits, I. In *Organic Sulphur Chemistry: Theoretical and Experimental Advances*; Bernardi, F., Csizmadia, I. G., Mangini, A., Eds.; Elsevier: Amsterdam, 1985; pp 191−245.

(25) (a) Burling, F. T.; Goldstein, B. M. *J. Am. Chem. Soc.* **1992**, *114*, 2313−2320. (b) Franchetti, P.; Cappellacci, L.; Grifantini, M.; Barzi, A.; Nocentini, G.; Yang, H.; O'Connor, A.; Jayaram, N. H.; Carrell, C.; Goldstein, B. M. *J. Med. Chem.* **1995**, *38*, 3829−3837. (c) Tanaka, R.; Oyama, Y.; Imajo, S.; Matsuki, S.; Ishiguro, M. *Bioorg. Med. Chem.* **1997**, *5*, 1389−1399. (d) Yamada, S.; Misono, T. *Tetrahedron Lett.* **2001**, *42*, 5497−5500. (e) Nagao, Y.; Hirata, T.; Goto, S.; Sano, S.; Kakehi, A.; Iizuka, K.; Shiro, M. *J. Am. Chem. Soc.* **1998**, *120*, 3104−3110. (f) Nagao, Y.; Iimori, H.; Goto, S.; Hirata, T.; Sano, S.; Chuman, H.; Shiro, M. *Tetrahedron Lett.* **2002**, *43*, 1709−1712. (g) Ángyán, J.; Poirier, R. A.; Kucsman, A.; Csizmadia, I. G. *J. Am. Chem. Soc.* **1987**, *109*, 2237−2245.

(26) Yassin, F. A. *Chem. Heterocycl. Compd.* **2009**, *45*, 35−41.

(27) Eyduran, F.; Oezyuerek, C.; Dilek, N.; Ocak Iskeleli, N.; Sendil, K. *Acta Crystallogr.* **2007**, *E63*, o2415−o2417.

(28) Sheldrick, G. M. *Acta Crystallogr.* **2008**, *A64*, 112−122.

(29) Farrugia, L. J. *J. Appl. Crystallogr.* **1999**, *32*, 837−838.

(30) Spek, A. L. *Acta Crystallogr.* **1990**, *A46*, C34.

(31) McKinnon, J. J.; Jayatilaka, D.; Spackman, M. A. *Chem. Commun.* **2007**, *37*, 3814−3816.

(32) Spackman, M. A.; McKinnon, J. J. *CrystEngComm* **2002**, *4*, 378−392.

(33) Sanner, M. F. *J. Mol. Graphics Modell.* **1999**, *17*, 57−61.

(34) Huey, R.; Morris, G. M.; Olson, A. J.; Goodsell, D. S. *J. Comput. Chem.* **2007**, *28*, 1145−1152.

(35) Morris, G. M.; Goodsell, D. S.; Hallidayetal, R. S. *J. Comput. Chem.* **1998**, *19*, 1639−1662.